

Oxygen-vacancy Bi_2O_3 nanosheets arrays with excellent rate capability and CoNi_2S_4 nanoparticles immobilized on N-doped graphene nanotubes as robust electrode materials for high-energy asymmetric supercapacitors

Jian Zhao^{a,b}, Zhenjiang Li^{a,b*}, Tong Shen^b, Xiangcheng Yuan^b,

Guanhao Qiu^a, Qingyan Jiang^c, Yusheng Lin^b, Guanying Song^a, Alan

Meng^{b*}, Qingdang Li^a

^a*Key Laboratory of Polymer Material Advanced Manufacturing Technology of Shandong Provincial College of Electromechanical Engineering, College of Sino-German Science and Technology, Qingdao University of Science and Technology, Qingdao 266061, Shandong, P. R. China.*

^b*State Key Laboratory Base of Eco-chemical Engineering, College of Chemistry and Molecular Engineering, College of Materials Science and Engineering, Qingdao University of Science and Technology, Qingdao 266042, Shandong, P. R. China.*

^c*Ocean College, Zhejiang University, Zhoushan 316021, Zhejiang, P. R. China.*

***Corresponding Author**

E-mail: zjli126@126.com

E-mail: mengalan@126.com

Calculations:

(1) The specific capacitances of the N-GNTs @OV-Bi₂O₃ NSAs or N-GNTs @CoNi₂S₄ NPs electrode calculated from GCD curves are obtained according to the following equation:

$$C = \frac{I\Delta t}{m\Delta V}$$

where I is the discharge current, Δt is the discharge time in GV test, m is the active material mass, and ΔV is the voltage window.

(2) The specific capacitance of the N-GNTs @OV-Bi₂O₃ NSAs // N-GNTs @CoNi₂S₄ NPs asymmetric supercapacitor (ASC) device can be got in accordance with the following equation:

$$C_{device} = \frac{I\Delta t}{M\Delta V}$$

Herein, I is the discharge current, Δt is the discharge time in GCD test, M is the total mass of both positive and negative electrodes, and ΔV is the voltage window of the device.

(3) Methods to calculate the energy and power density of the ASC device:

$$E = \frac{1}{2} C_{device} \Delta V^2 ; P = \frac{E}{t}$$

Here, C_{device} is the specific capacitance of the device, ΔV is the potential window, and t is the discharge time.

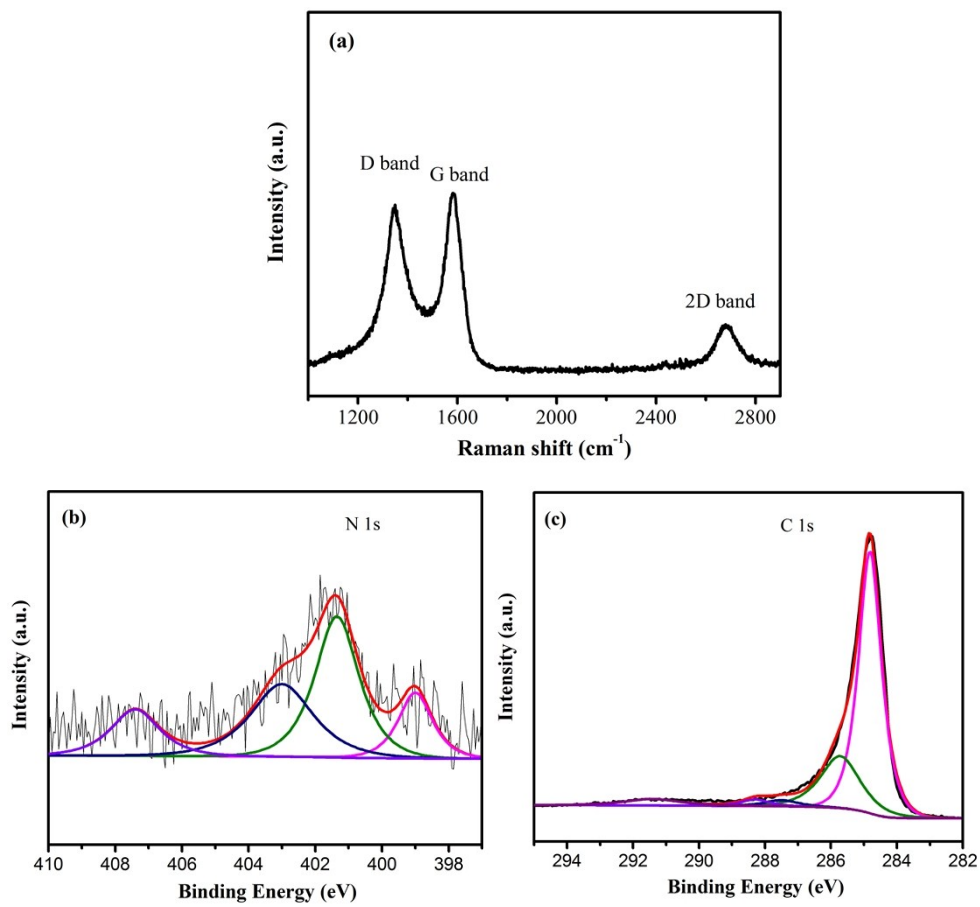


Fig. S1 The Raman spectrum (a), high-resolution XPS N1s (b) and C1s (c) of the pure N-GNTs.

Tab. S1 Atomic percentage of each element in the N-GNTs obtained from the XPS spectra.

Element name	atomic (%)
C	97.11
N	2.07
O	0.82

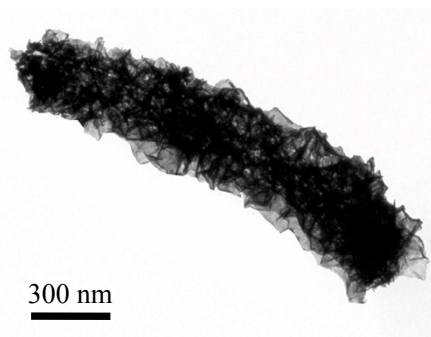


Fig. S2 TEM image of N-GNT@Bi₂O₃ NSAs

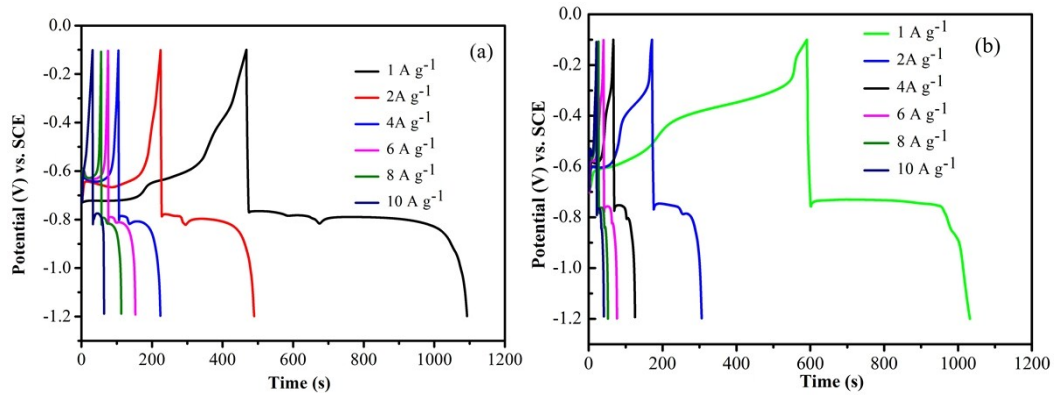


Fig. S3 The GCD measurements of the N-GNTs@Bi₂O₃ NSAs (a) and Bi₂O₃ NSAs (b).

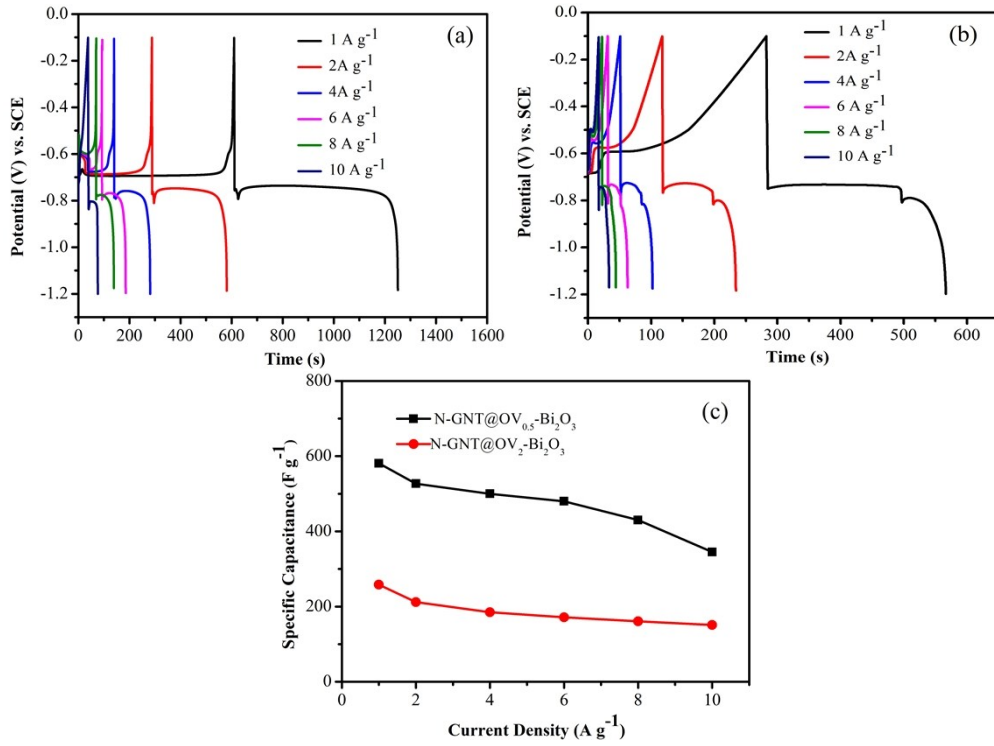


Fig. S4 GCD curves of N-GNTs@OV_{0.5}-Bi₂O₃ (a) and N-GNTs@OV₂-Bi₂O₃ (b) at various current densities, and their specific capacitance values versus different current densities (c)

Tab. S2 Comparison of the electrochemical properties of the as-fabricated N-GNT @OV-Bi₂O₃ NNAs with previously reported negative electrode materials.

Material	Fabrication method	current collector	electrolyte	Specific capacitance (F g ⁻¹)	Rate performance	Reference
Bi ₂ O ₃	Hydrothermal	Ni foam	6M KOH	447 (2A g ⁻¹)	260 (10 A g ⁻¹)	S1
FeOOH	electrodeposition	Polyamide Nanofiber Film	2M LiCl	315 (0.5 A g ⁻¹)	194 (10 A g ⁻¹)	S2
Bi ₂ S ₃	Hydrothermal and calcination	S-NCNF	6M KOH	466 (1 A g ⁻¹)	299 (8 A g ⁻¹)	S3
Fe ₂ O ₃ QDs	thermal decomposition	Ti Foil	1M Na ₂ SO ₄	347 (10 mV s ⁻¹)	140 (160 mV s ⁻¹)	S4
rGO/Fe ₂ O ₃	Hydrothermal	Ni foam	2M KOH	469.5 (4 A g ⁻¹)	132.4 (16 A g ⁻¹)	S5
WO ₃	calcination	GCE	0.5M H ₂ SO ₄	508 (1 A g ⁻¹)	332.2 (20 A g ⁻¹)	S6
rGO/Fe ₂ O ₃	solvothermal	Ni foam	4M KOH	520 (1 A g ⁻¹)	443 (25 A g ⁻¹)	S7
NiNTAs@Fe ₂ O ₃	electrodeposition and calcination	Ti Foil	1M Na ₂ SO ₄	418.7 (10 mV s ⁻¹)	—	S8
Fe ₂ O ₃ -P	Hydrothermal and calcination	carbon cloth	1M Na ₂ SO ₄	369 (1 mV s ⁻¹)	—	S9
MoS ₂ /GNS	Hydrothermal and calcination	Ni foam	1M Na ₂ SO ₄	320 (2 A g ⁻¹)	~170 (10 A g ⁻¹)	S10
N-GNT@OV-Bi₂O₃	Hydrothermal	Graphite wafer	6M KOH	643 (1 A g⁻¹)	450 (10 A g⁻¹)	In this work

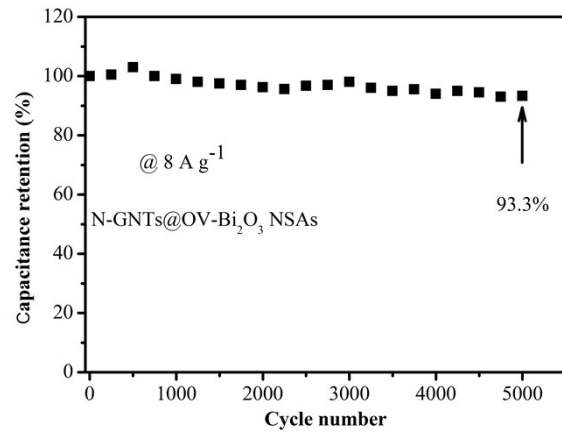


Fig. S5 Cyclic stability of the N-GNTs@OV-Bi₂O₃ NSAs negative electrode materials over 5000 cycles at 8 A g⁻¹.

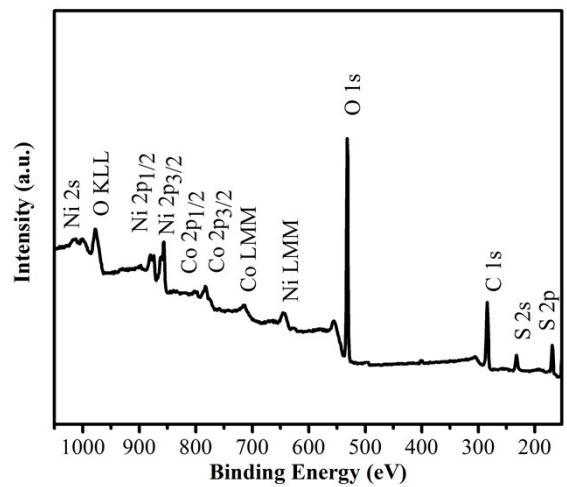


Fig. S6 XPS survey spectrum of N-GNTs@CoNi₂S₄ NPs

Tab. S3 Electrochemical performances comparison of the as-prepared N-GNT @CoNi₂S₄ HNAs with other Ni-Co compound based positive electrodes fabricated by different methods.

Material	Fabrication method	current collector	electrolyte	Specific capacitance (F g ⁻¹)	Rate performance	Reference
NiS	Solvothermal and calcination	Carbon substrate	2M KOH	874.5 (1 A g ⁻¹)	454.5 (20 A g ⁻¹)	S11
Ni-Co-S@Ni-W-O	Hydrothermal and calcination	Ni foam	6M KOH	1988 (2 A g ⁻¹)	1500 (30 A g ⁻¹)	S12
CoNi ₂ S ₄	Chemical deposition	Ni foam	2M KOH	1530 (1 A g ⁻¹)	1346 (8 A g ⁻¹)	S13
NiCo ₂ O ₄ /CNT	Calcination	Ni foam	2M KOH	1596 (1 A g ⁻¹)	1406 (10 A g ⁻¹)	S14
NiCo ₂ S ₄ /Co ₉ S ₈	Hydrothermal	Ni foam	6M KOH	749 (4 A g ⁻¹)	620 (15 A g ⁻¹)	S15
NiGa ₂ O ₄ NAs	Hydrothermal and calcination	Ni foam	6M KOH	1508 (1 A g ⁻¹)	960 (20 A g ⁻¹)	S16
Ni ₃ S ₂ @NiS	Hydrothermal	Ni foam	6M KOH	1158 (2 A g ⁻¹)	670 (50 A g ⁻¹)	S17
NiCo ₂ O ₄	Hydrothermal and calcination	Carbon cloth	2M KOH	1055 (0.4 A g ⁻¹)	483 (10 A g ⁻¹)	S18
Co ₃ O ₄ @NiCo ₂ O ₄	Hydrothermal and calcination	Carbon cloth	2M KOH	1450 (1 A g ⁻¹)	1374 (3 A g ⁻¹)	S19
H-3DRG@NiCo-LDH	Hydrothermal	Ni foam	2M KOH	1634 (0.5 A g ⁻¹)	1260 (20 A g ⁻¹)	S20
N-GNT@CoNi ₂ S ₄	Hydrothermal and sulfuration	Graphite wafer	6M KOH	2142 (2.5 A g ⁻¹)	1785 (25 A g ⁻¹)	In this work

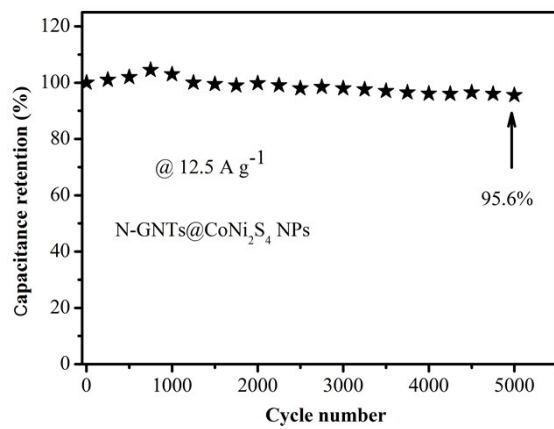


Fig. S7 Cyclic stability of the N-GNTs@ CoNi₂S₄ NPs positive electrode materials over 5000 cycles at 12.5 A g⁻¹.

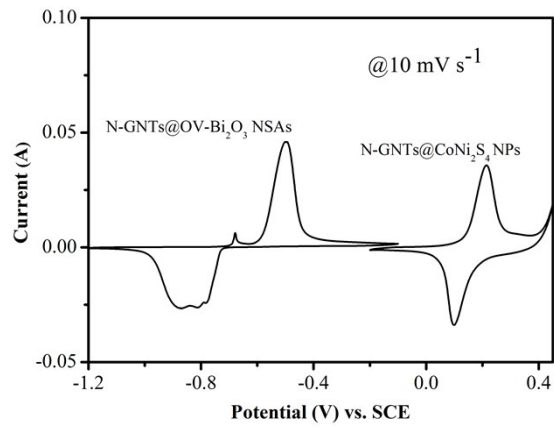


Fig. S8 CV curves of the N-GNTs@OV-Bi₂O₃ NSAs and N-GNTs@CoNi₂S₄ NPs at 10 mV s⁻¹.

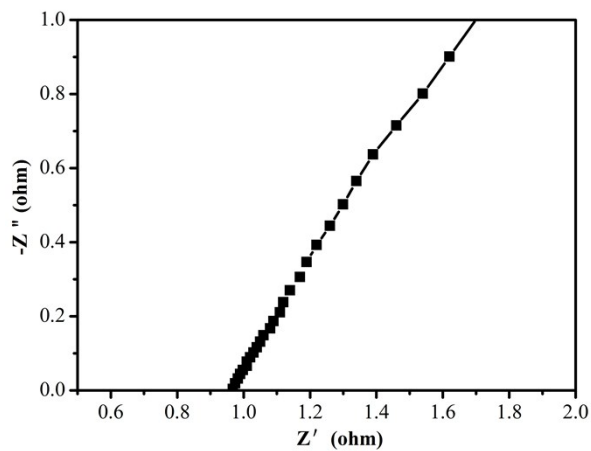


Fig. S9 The Nyquist plot of the assembled N-GNTs@OV-Bi₂O₃ NSAs//N-GNTs@CoNi₂S₄ NPs

asymmetric supercapacitor.

Tab. S4 The maximum specific energy density comparison of our device with the reported state-of-the-art ASC devices with other nanostructures as electrode materials.

ASC devices	Cell voltage (V)	electrolyte	Maximun energy density (Wh kg ⁻¹)	Reference
CoNi ₂ S ₄ /CNT//Fe ₂ O ₃ /CNT	1.7	2 M KOH	50 (0.847 kW kg ⁻¹)	S13
NiCo ₂ O ₄ /NC	1.6	PVA/KOH	31.9 (2.9 kW kg ⁻¹)	S18
(Ni _{0.1} Co _{0.9}) ₉ Se ₈ @CFC//rGO@CFC	1.55	PVA/KOH	17.0 (3.1 kW kg ⁻¹)	S21
ESCNF@Bi ₂ O ₃ //CF@NiCo ₂ O ₄	1.9	1M KOH	25.1 (0.786 kW kg ⁻¹)	S22
LDH-NPs/CH-NWs//AC	1.6	6M KOH	58.9 (0.4 kW kg ⁻¹)	S23
Ni ₃ S ₂ /CoNi ₂ S ₄ /NF//AC/NF	1.7	6M KOH	50.7 (1.59 kW kg ⁻¹)	S24
NiCo ₂ O ₄ @Ni _x Co _y MoO ₄ //AC	1.5	PVA-KOH	64.7 (0.75 kW kg ⁻¹)	S25
Co ₃ O ₄ /ZnCo ₂ O ₄ /CuO//AC	1.6	PVA-KOH	35.8 (0.80 kW kg ⁻¹)	S26
Ni(OH) ₂ -CoQD//rGO	1.45	2M KOH	46 (0.14 kW kg ⁻¹)	S27
NiCo ₂ S ₄ /NCF//OMC/NCF	1.6	6M KOH	45.5 (0.5 kW kg ⁻¹)	S28
N-GNT@CoNi₂S₄//N-GNT@OV-Bi₂O₃	1.6	6M KOH	86.6 (1.6 kW kg⁻¹)	In this work

Tab. S5 Cycle performance comparison of the assembled ASC with other state-of-the-art ASC devices with various positive and negative electrodes.

ASC devices	Cell voltage	electrolyte	Cycle performance	Reference
$\text{Bi}_2\text{O}_3/\text//\text{MnCO}_3\text{QDs}/\text{NiH-Mn-CO}_3$	1.5	6M KOH	81% retention after 5000 cycles	S1
$\text{CuCo}_2\text{O}_4/\text{CuO/rGO/Fe}_2\text{O}_3$	1.6	2M KOH	83% retention after 5000 cycles	S5
$\text{Ni(OH)}_2\text{-CoQD//RGO}$	1.45	2M KOH	84.1% retention after 5000 cycles	S27
$\text{NiCo}_2\text{S}_4/\text{NCF //OMC/NCF}$	1.6	6M KOH	70.4% retention after 10000 cycles	S28
$\text{MnO}_2/\text{CNT//CNT/PPy}$	1.5	KOH	80% retention after 5000 cycles	S29
$\text{HP-CF-NiCo}_2\text{S}_4/\text{HP-CF-Fe}_2\text{O}_3$	1.7	3M KOH	81.1% retention after 1000 cycles	S30
$\text{MnCo}_2\text{O}_4@\text{Ni(OH)}_2/\text//\text{AC}$	1.6	2M KOH	90% retention after 2500 cycles	S31
$\text{PEDOT}@\text{MnO}_2/\text{C@Fe}_3\text{O}_4$	2	PVA- LiCl	80% retention after 800 cycles	S32
$\text{NiO//Fe}_2\text{O}_3$	1.8	2M KOH	68% retention after 5000 cycles	S33
$\text{FeOOH/PPy@CF//MnO}_2/\text{CF}$	1.6	PVA/LiCl	82% retention after 5000 cycles	S34
N-GNTs@CoNi₂S₄/N-GNTs@OV-Bi₂O₃	1.6	6M KOH	97% and 85.5% retention after 6000 and 10000 cycles, respectively	In this work

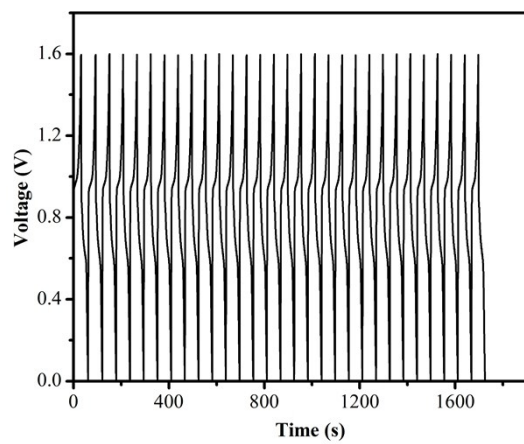


Fig. S10 The GCD curves of the first 30 cycles for the assembled device.

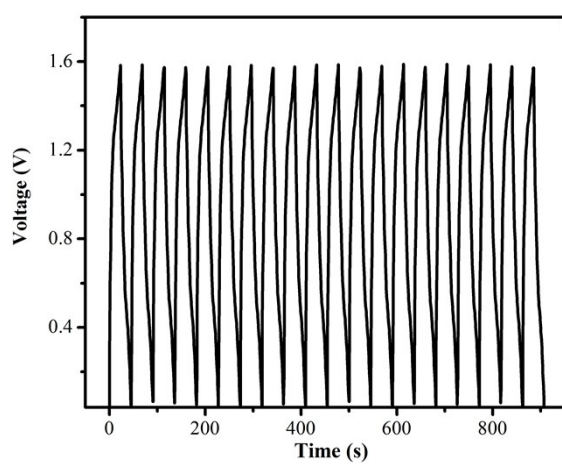


Fig. S11 The GCD curves of the last 20 cycles for the assembled device.

The operation mechanism of positive and negative electrodes is specifically expounded as follows.

In KOH aqueous electrolyte, the OH⁻ ions are proposed to be repeatedly embedded/detached into/from the active materials for oxidation and reduction reactions. Concretely, when the assembled ASC is charged, the positive electrode N-GNTs@CoNi₂S₄ is oxidized, representing as CoNi₂S₄ + 2OH⁻ → CoS_{2x}OH + Ni₂S_{4-2x}OH + 2e⁻,^{S35,S36} and the negative electrode N-GNTs@OV-Bi₂O₃ conducts the reduction reaction according to the process of Bi₂O₃ + H₂O + 2e⁻ → Bi₂O₂ + 2OH⁻, Bi₂O₂ + 2H₂O + 4e⁻ → 2Bi + 4OH⁻.^{S1,S37} In terms of the discharging procedure, the reactions occur backward. It can be seen that during the charging/discharging process, as for the positive and negative electrode, one consumes OH⁻, and the other generates OH⁻. Thus, both the electrodes store the same OH⁻ group, and after charging/discharging process, the electrolyte can still make neutral. It is consistent with the operation mechanism of previous reported asymmetric supercapacitor devices with different positive/negative electrode materials in KOH aqueous solution.^{S5,S38-S41}

References

- S1 N. M. Shinde, Q. X. Xia, J. M. Yun, R. S. Mane and K. H. Kim, *ACS Appl. Mater. Interfaces*, 2018, **10**, 11037.
- S2 T. T. Gao, Z. Zhou, J. Y. Yu, D. X. Cao, G. L. Wang, B. Ding and Y. J. Li, *ACS Appl. Mater. Interfaces*, 2018, **10**, 23834.
- S3 W. Zong, F. L. Lai, G. J. He, J. R. Feng, W. Wang, R. Q. Lian, Y. E. Miao, G. C. Wang, I. P. Parkin and T. X. Liu, *Small*, 2018, **14**, 1801562.
- S4 H. Xia, C. Y. Hong, B. Li, B. Zhao, Z. X. Lin, M. B. Zheng, S. V. Savilov and S. M. Aldoshin, *Adv. Funct. Mater.*, 2015, **25**, 627.
- S5 Y. D. Wang, C. Shen, L. Y. Niu, R. Z. Li, H. T. Guo, Y. X. Shi, C. Li, X. J. Liu and Y. Y. Gong, *J. Mater. Chem. A*, 2016, **4**, 9977.
- S6 D. Mandal, P. Routh and A. K. Nandi, *Small*, 2018, **14**, 1702881.
- S7 Y. Wang, Z. X. Chen, T. Lei, Y. F. Ai, Z. K. Peng, X. Y. Yan, H. Li, J. J. Zhang, Z. M. M. Wang and Y. L. Chueh, *Adv. Energy Mater.*, 2018, **8**, 1703453.
- S8 Y. Li, J. Xu, T. Feng, Q. F. Yao, J. P. Xie and H. Xia, *Adv. Funct. Mater.*, 2017, **27**, 1606728.
- S9 H. F. Liang, C. Xia, A. H. Emwas, D. H. Anjum, X. H. Miao and H. N. Alshareef, *Nano Energy*, 2018, **49**, 155.
- S10 X. Yang, H. Niu, H. Jiang, Q. Wang and F. Y. Qu, *J. Mater. Chem. A*, 2016, **4**, 11264.
- S11 X. Ma, L. Zhang, G. C. Xu, C. Y. Zhang, H. J. Song, Y. T. He, C. Zhang and D. Z. Jia, *Chemical Engineering Journal*, 2017, **22**, 320.
- S12 W. D. He, Z. F. Liang, K. Y. Ji, Q. F. Sun, T. Y. Zhai and X. J. Xu, *Nano*

Research, 2018, **11**, 1415.

- S13 X. Cao, J. He, H. Li, L. P. Kang, X. X. He, J. Sun, R. B. Jiang, H. Xu, Z. B. Lei and Z. H. Liu, *Small*, 2018, **14**, 1800998.
- S14 P. Wu, S. Cheng, M. Yao, L. Yang, Y. Zhu, P. Liu, O. Xing, J. Zhou, M. Wang and H. Luo, *Adv. Funct. Mater.*, 2017, **27**, 1702160.
- S15 L. R. Hou, Y. Y. Shi, S. q. Zhu, M. Rehan, G. Pang, X. G. Zhang and C. Z. Yuan, *J. Mater. Chem. A*, 2017, **5**, 133.
- S16 S. Liu, K. S. Hui, K. N. Hui, H. F. Li, K. W. Ng, J. Xu, Z. Tang and S. C. Jun, *J. Mater. Chem. A*, 2017, **5**, 19046.
- S17 W. Li, S. L. Wang, L. P. Xin, M. Wu and X. J. Lou, *J. Mater. Chem. A*, 2016, **4**, 7700.
- S18 C. Guan, X. M. Liu, W. N. Ren, X. Li, C. W. Cheng and J. Wang, *Adv. Energy Mater.*, 2017, **12**, 1602391.
- S19 X. Wu, Z. C. Han, X. Zheng, S. Y. Yao, X. Yang and T. Y. Zhai, *Nano Energy*, 2017, **31**, 410.
- S20 K. Q. Qin, L. P. Wang, S. W. Wen, L. C. Diao, P. Liu, J. J. Li, L. Y. Ma, C. S. Shi, C. Zhong, W. B. Hu, E. Z. Liu and N. Q. Zhao, *J. Mater. Chem. A*, 2018, **6**, 8109.
- S21 P. Y. Yang, Z. Y. Wu, Y. C. Jiang, Z. C. Pan, W. C. Tian, L. Jiang and L. F. Hu, *Adv. Energy Mater.*, 2018, **8**, 1801392.
- S22 L. Li, X. T. Zhang, Z. G. Zhang, M. Y. Zhang, L. J. Cong, Y. Pan and S. Y. Lin, *J. Mater. Chem. A*, 2016, **4**, 16635.

- S23 J. Yang, C. Yu, X. M. Fan and J. S. Qiu, *Adv. Energy Mater.*, 2014, **4**, 1400761.
- S24 W. D. He, C. G. Wang, H. Q. Li, X. L. Deng, X. J. Xu and T. Y. Zhai, *Adv. Energy Mater.*, 2017, **7**, 1700983.
- S25 P. X. Sun, W. D. He, H. C. Yang, R. Y. Cao, J. M. Yin, C. G. Wang and X. J. Xu, *Nanoscale*, 2018, **10**, 19004.
- S26 S. S. Zhou, Z. C. Ye, S. Z. Hu, C. Hao, X. H. Wang, C. Huang and F. S. Wu, *Nanoscale*, 2018, **10**, 15771.
- S27 D. W. Shi, L. Y. Zhang, N. D. Zhang, Y. W. Zhang, Z. G. Yu, H. Gong, *Nanoscale*, 2018, **10**, 10554.
- S28 L. F. Shen, J. Wang, G. Y. Xu, H. S. Li, H. Dou and X. G. Zhang, *Adv. Energy Mater.*, 2015, **5**, 1400977.
- S29 J. L. Yu, W. B. Lu, J. P. Smith, K. S. Booksh, L. H. Meng, Y. D. Huang, Q. W. Li, J. H. Byun, Y. S. Oh, Y. H. Yan and T. W. Chou, *Adv. Energy Mater.*, 2017, **7**, 1600976.
- S30 J. Z. Chen, J. L. Xu, S. Zhou, N. Zhao and C. P. Wong, *Nano Energy*, 2016, **25**, 193.
- S31 Y. Zhao, L. F. Hu, S. Y. Zhao and L. M. Wu, *Adv. Funct. Mater.*, 2016, **26**, 4085.
- S32 J. F. Sun, Y. Huang, C. X. Fu, Y. Huang, M. S. Zhu, X. M. Tao, C. Y. Zhi and H. Hu, *J. Mater. Chem. A*, 2016, **4**, 14877.
- S33 Q. Q. Tang, W. Q. Wang and G. C. Wang, *J. Mater. Chem. A*, 2015, **3**, 6662.
- S34 X. F. Gong, S. H. Li and P. S. Lee, *Nanoscale*, 2017, **9**, 10794.
- S35 W. Chen, C. Xia and H. N. Alshareef, ACS Nano, 2014, 8, 9531.**

- S36 J. W. Xiao, L. Wan, S. H. Yang, F. Xiao and S. Wang, *Nano Lett.*, 2014, 14, 831.
- S37 L. Li, X. T. Zhang, Z. G. Zhang, M. Y. Zhang, L. J. Cong, Y. Pan and S. Y. Lin, *J. Mater. Chem. A*, 2016, 4, 16635.
- S38 K. A. Owusu, L. B. Qu, J. T. Li, Z. Y. Wang, K. N. Zhao, C. Yang, K. M. Hercule, C. Lin, C. W. Shi, Q. L. Wei, L. Zhou and N L. Q. Mai, *Nature Comm.*, 2017, 8, 14264.
- S39 W. K. Zhang, B. Zhao, Y. L. Yin, T. Yin, J. Y. Cheng, K. Zhan, Y. Yan, J. H. Yang and J. Q. Li, *J. Mater. Chem. A*, 2016, 4, 19026
- S40 T. Li, W. L. Zhang, L. Zhi, H. Yu, L. Q. Dang, F. Shi, H. Xu, F. Y. Hu, Z. H. Liu, Z. B. Lei, J. S. Qiu, *Nano Energy*, 2016, 30, 9.
- S41 F. Li, H. Chen, X. Y. Liu, S. J. Zhu, J. Q. Jia, C. H. Xu, F. Dong, Z. Q. Wen and Y. X. Zhang, *J. Mater. Chem. A*, 2016, 4, 2096.